Journal of Biomedical Optics

SPIEDigitalLibrary.org/jbo

Ultrafast laser ablation and machining large-size structures on porcine bone

Ran An
Ghadeer W. Khadar
Emilia I. Wilk
Brent Emigh
Harold K. Haugen
Gregory R. Wohl
Brett Dunlop
Mehran Anvari
Joseph E. Hayward
Qiyin Fang

SPIE

Ultrafast laser ablation and machining large-size structures on porcine bone

Ran An,[a] Ghadeer W. Khadar,[a] Emilia I. Wilk,[a] Brent Emigh,[b] Harold K. Haugen,[a,c] Gregory R. Wohl,[d,e] Brett Dunlop,[f] Mehran Anvari,[g] Joseph E. Hayward,[b] and Qiyin Fang[a,e]

[a]McMaster University, Department of Engineering Physics, 1280 Main Street West, Hamilton, Ontario L8S 4L7, Canada
[b]McMaster University, Department of Medical Physics and Applied Radiation Sciences, 1280 Main Street West, Hamilton, Ontario L8S 4L7, Canada
[c]McMaster University, Department of Physics and Astronomy, 1280 Main Street West, Hamilton, Ontario L8S 4L7, Canada
[d]McMaster University, Department of Mechanical Engineering, 1280 Main Street West, Hamilton, Ontario L8S 4L7, Canada
[e]McMaster University, School of Biomedical Engineering, 1280 Main Street West, Hamilton, Ontario L8S 4L7, Canada
[f]McMaster University, Division of Orthopedic Surgery, Department of Surgery, 1280 Main Street West, Hamilton, Ontario L8S 4L7, Canada
[g]McMaster University, Division of General Surgery, Department of Surgery, 1280 Main Street West, Hamilton, Ontario L8S 4L7, Canada

Abstract. When using ultrafast laser ablation in some orthopedic applications where precise cutting/drilling is required with minimal damage to collateral tissue, it is challenging to produce large-sized and deep holes using a tightly focused laser beam. The feasibility of producing deep, millimeter-size structures under different ablation strategies is investigated. X-ray computed microtomography was employed to analyze the morphology of these structures. Our results demonstrated the feasibility of producing holes with sizes required in clinical applications using concentric and helical ablation protocols. [DOI: 10.1117/1.JBO.18.7.070504]

Keywords: laser ablation; orthopedic applications.

Paper 130276LR received Apr. 24, 2013; revised manuscript received Jun. 19, 2013; accepted for publication Jun. 27, 2013; published online Jul. 24, 2013.

1 Introduction

Compared with conventional mechanical cutting/drilling tools, the laser has great potential in surgical applications since it is noncontact, minimally invasive, and easy to integrate with real-time feedback mechanisms.[1–3] Although most work on laser ablation mechanisms and its clinical applications are for soft tissue,[4–10] a number of studies have been reported on hard-tissue ablation and machining, where they demonstrated different ablation characteristics and underlying mechanisms.[1,11–14] Besides dental applications, ablation of regular bone has also been investigated for potential applications in cosmetic[15,16] and orthopedic surgery.[17,18] The ablation in these studies is mostly based on thermal effects that are associated with significant collateral damage.[19,20] Benefiting from the plasma-induced ablation mechanism, ultrafast pulsed lasers emerge as a promising candidate for hard-tissue ablation because they offer high resolution with minimal thermal-related damage in the collateral tissues.[21–24] On the other hand, tight focusing and small volume of tissue removal are typical in ultrafast laser ablation, which make it difficult to produce large structures needed in clinical applications.

We recently studied a number of parameters in ultrafast laser ablation using porcine vertebral bone, including ablation threshold and the incubation effect.[24] In this communication, we conducted proof-of-principle studies to explore the potential of ultrafast lasers to produce millimeter-scale holes using different ablation protocols. Porcine vertebral bone was used since it has similar bone density, composition, and mechanical properties as human bone.[25] In order to offer better reference for potential clinical applications, the porcine bone sample surface was kept unaltered (i.e., not polished).

2 Experimental Setup and Results

The ablation experiments were carried out in a customized ultrafast laser machining setup as shown in Fig. 1. A detailed description of this setup can be found in previous publications[24,26] and is briefly depicted here. Femtosecond laser pulses from a Ti:Sapphire oscillator (Tsunami, Spectra Physics) were amplified to maximum pulse energy of ~400 to 500 μJ and pulse duration of 170 fs at a repetition rate of 1 kHz. For the results reported here, the wavelength of the laser was set at 800 nm. The collimated beam diameter was reduced to a final $1/e^2$ diameter of 4.4 mm through a telescope. The combination of a polarizer and a half-wave plate was used to adjust the pulse energy. The laser exposure time (i.e., number of pulses used in ablation) was adjusted by a computer-controlled mechanical shutter (VS25S2S1, Uniblitz, Rochester, New York). A plano-convex lens ($f = 12.5$ cm, BK7, Thorlabs, Newton, New Jersey) focused the collimated beam down to a $1/e^2$ spot size diameter of 30.2 μm. The bone sample was placed in a sealed glass vial during ablation to prevent the biological residue from spreading outside the environment. A glass microscope coverslip was used to seal the vial while allowing the ablation beam to pass through. Horizontal scanning of the sample is achieved using an $X - Y$ translational stage (UTM100PP.1, Newport, Irvine, California), while vertical scanning is achieved by moving the focusing lens through a linear (Z) translation stage (MFN25PP, Newport).

The experimental protocol was approved by the Animal Research Ethics Board of McMaster University. Vertebrae bone specimens were harvested from skeletally immature pigs obtained from a local butcher in Hamilton, Ontario. The soft tissue and periosteum were removed and a handsaw was used to cut bone samples into smaller sizes (10×10 mm^2, 5 to 8 mm in height). The samples included both the outer cortical layer (1- to 3-mm thick) as well as the underlying cancellous bone (~5 mm). The bone specimens were stored in ice immediately following harvest and the laser ablation experiments were carried out soon after. After the experiments, the ablated specimens were stored at −20°C in a freezer for a few days and then examined by x-ray microcomputed tomography (μCT, GE Medical Systems, London, ON MicroCT eXplore RS80; isometric resolution of 27 μm).

In orthopedic applications, such as pedicle screw pilot-hole drilling, prosthetic implantation, and osteotomies, it is necessary to produce straight holes on the scale of millimeters to even

Address all correspondence to: Qiyin Fang, McMaster University, Department of Engineering Physics, 1280 Main Street West, Hamilton, Ontario L8S 4L7, Canada. Tel.: 9055259140; Fax: 905.528.5406; E-mail: qiyin.fang@mcmaster.ca

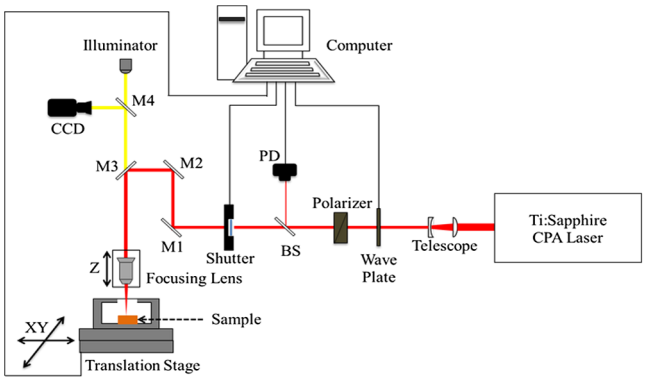

Fig. 1 Schematic of laser ablation setup. The sample scanning is achieved by moving the chamber using an $X-Y$ translation stage and moving the focusing lens with a Z stage. The CCD camera monitored the ablation process to ensure laser-sample alignment. CPA, chirped-pulse amplifier; BS, beam-splitter; PD, photodiode; M1 and M2 are high-reflection mirrors, M3 is a dichroic mirror, and M4 is a beam splitter.

centimeters in depth,[27,28] which means removal of relatively large volumes of bone tissue in comparison to the ablation diameter of the laser (~30 μm) in the case of tightly focused ultrafast lasers. To fabricate structures on a millimeter scale, we investigated two scanning protocols: concentric circular and helical scanning.

A concentric circle scanning/milling protocol was first used to produce larger-diameter holes. The fluence was set to 19.3 J/cm^2, and the scanning speed was set at 500 μm/s. Figure 2(d) illustrates the concentric circle scanning protocol: a continuous scanning of 20 concentric circles was carried out with the laser focus aligned right on the sample surface for each layer. Each successive circle had a radius increase of 25 μm.

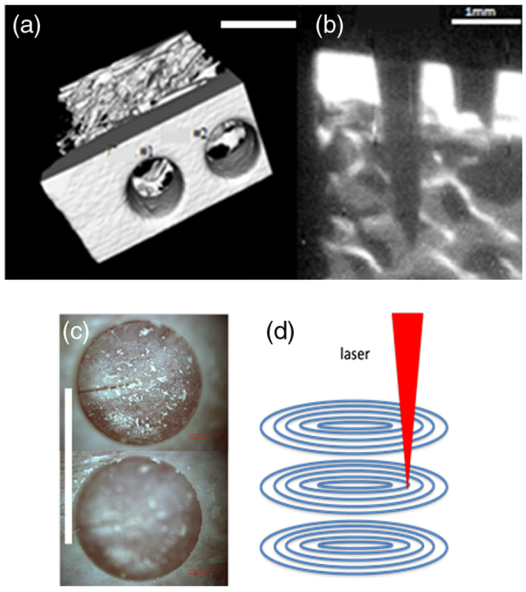

Fig. 2 Images of through holes ablated by using the concentric circle approach. (a) Three-dimensional μCT reconstructed images of the holes produced on the porcine bone. (b) A cross-section view of the same μCT image showing a 3-mm-deep hole (note that this cross-section view was not chosen at the maximum depth of the hole) penetrating through the cortical layer (~1 mm thick). (c) Top-view optical micrographs of the shallower hole with the focus on the sample surface and the hole bottom, respectively. The scale bars are all 1 mm in length, while the magnification factors are different in each of the three images. (d) Illustration of concentric circle drilling protocol.

Compared to the actual ablation diameter of the laser beam (~30 μm), this increment was chosen to ensure sufficient beam overlap between circular passes. After one layer was machined then the laser focus was moved downward by 200 μm to machine successive layers. Different hole depths could be machined by controlling the number of removed layers. A total of 32 holes were ablated under the same laser parameters. Figure 2(a) and 2(b) show reconstructed μCT images of two typical holes through the cortical layer with two different view angles. The first hole (#1) had 20 layers and the second hole (#2) had 10 layers, corresponding to hole depths of 4 and 2 mm, respectively. The machining time was 28 and 14 min, respectively. From analysis of μCT scan images, the hole depths were measured to be 3.81 and 1.51 mm, which are shallower than expected due to debris deposited on the bottom of the holes.[29] The side walls of the holes on the cortical bone showed smooth surface and were free of any cracks or thermal damage. We were not able to image the crater side wall clearly on cancellous bones because of difficulties in differentiating the ablation hole from native pores in the less dense and porous trabecular bone using the μCT images.

In Fig. 2(b), the cross-sectional images of both holes are shown. One can see the shape of the holes became tapered, especially at the deep end of the deeper hole. This is because part of the focusing laser beam was blocked by the side wall when the focal plane was well below the surface at the deep end of the hole. Figure 2(c) shows the top view optical microscopy image of the shallower hole, which did not cut through the cortical layer. By focusing on the bone surface and bottom, one can see that the bone tissue was removed completely and all the holes showed smooth edges and were free of thermal damage to the tissue outside the perimeter of the hole.

In clinic applications, the time allowed for producing such holes should be limited to 1 min or less. In the concentric circle drilling, it took 28 min to produce the deeper holes in Fig 2. Therefore, another ablation protocol using spiral helical scan pattern was investigated to reduce ablation time. In this helical scan protocol, as illustrated in Fig. 3(c), only the outside perimeter of the hole is ablated by a spiral pattern moving downward. In principle, the time required for helical scanning linearly depends on the size of the hole, which may save significant operating time.

Three coaxial helices diameters of 900, 950, and 1000 μm were investigated with the fluence of the laser set to 2.6 J/cm^2 and a scanning speed of 500 μm/s. Each helix included 40 full circles and a pitch Δz of 100 μm between successive circles. The total machining time was <13 min. Figure 3(a) shows a three-dimensional reconstructed image from μCT scans of the laser-machined trench and pillar on an incomplete sample. From the two-dimensional cross-sectional image in

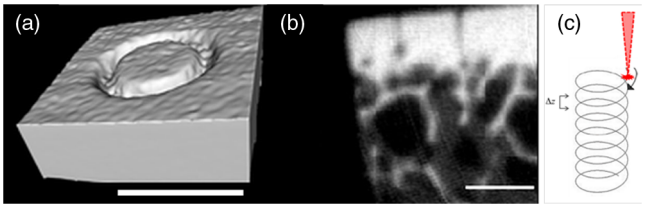

Fig. 3 μCT images of an incomplete hole produced by helix circle approach. (a) Three-dimensional reconstructed images of an incomplete hole on the porcine bone. (b) Two-dimensional cross-sectional view of the ablated hole, showing the pillar in the middle. The scale bars are 1 mm in length, while the two images are of different magnification factors. (c) Illustration of the helix circle ablation protocol.

the lower-right corner of Fig. 3(b), where the helix is cutting through the cortical layer, the trench bottom appeared to be very close to the cancellous bone if not already ablated into it. However, due to the resolution limitation of the μCT (27 μm), it is hard to tell the exact length of the trench. Since the cancellous bone was porous, it would be easy to remove the cortical bone pillar to form a hole. This suggests the helical drilling method would be a faster way to make holes on cortical bone, although the technique to remove the pillar safely in clinical applications remains to be studied. In a second experiment, by increasing the laser fluence to 19.7 J/cm^2 and the scanning speed to 800 μm/s, we were able to reduce the vertical pass number to 12 and increase the separation of successive pass to 500 μm. The total machining time then dropped significantly to <2.5 min.

3 Summary and Discussion

We have investigated two drilling strategies which both demonstrated the capability to produce millimeter-size holes through the cortical bone. The advantages of using lasers to produce these holes include the feasibility of incorporating real-time sensing and feedback mechanisms for high accuracy and precision,[3,30] which is critical to applications such as pedicle screw placement. There are several issues in using laser ablation on hard tissue, such as thermal damage to collateral tissue, shallow penetration depth and difficulty in producing large-diameter and deep holes, and time-consuming drilling time.

Ultrafast pulsed lasers have shown great promise as an alternative bone drilling technique owing to the advantages of high precision and minimal thermal collateral damage. We investigated different drilling strategies for holes of millimeter sizes, and our results indicate that it is feasible to use ultrafast laser ablation in bone.

Since bone is reported to have smaller thermal conductivity and diffusivity, local thermal damage is an issue in laser ablation of bone.[31] In ultrafast ablation, thermal damage is usually limited because the dominate ablation mechanism is not thermal based and the total deposited energy is low.[21] In our results, including those reported earlier using similar parameters,[24] very little thermal damage was observed on the side of the crater.

Although the ablation time is quite long in the results presented here, it should be noted that a 1-kHz repetition rate laser was used in this feasibility study. It is reasonable to expect that ablation time can be significantly reduced when using emerging ultrafast fiber lasers with repetition rate into 100s kHz to MHz regime.

Acknowledgments

This project is supported in part by the Natural Sciences and Engineering Research Council of Canada through the Discovery and Research Tools and Instrument Program (Q.F. and H.H.), Canada Foundation for Innovation (G.W.), and the Ontario Ministry of Research and Innovation (G.W. and Q.F.).

References

1. R. H. Stern, J. Vahl, and R. F. Sognnaes, "Lased enamel: ultrastructural observations of pulsed carbon dioxide laser effects," *J. Dent. Res.* **51**(2), 455–460 (1972).
2. T. Vo-Dihn, *Biomedical Photonics Handbook*, CRC Press, Boca Raton, FL (2002).
3. F. Stelzle et al., "In vivo optical tissue differentiation by diffuse reflectance spectroscopy: preliminary results for tissue-specific laser surgery," *Surg. Innov.* **19**(4), 385–393 (2012).
4. M. B. McDonald et al., "Excimer laser ablation human eye," *Arch Ophthalmol.* **107**(5), 641–642 (1989).
5. A. Vogel and V. Venugopalan, "Mechanisms of pulsed laser ablation of biological tissues," *Chem. Rev.* **103**(2), 577–644 (2003).
6. Q. Fang and X. H. Hu, "Modeling of skin-tissue ablation by nanoseconds laser pulses from ultra violet to near-inferred and comparison with experimental results," *IEEE J. Quantum Electron.* **40**(1), 69–77 (2004).
7. X. H. Hu et al., "In vivo study of intradermal focusing for tattoo removal," *Laser Med. Sci.* **17**(3), 154–164 (2002).
8. X. H. Hu et al., "Mechanism study of porcine skin ablation by nanosecond laser pulses at 1064, 532, 266, and 213 nm," *IEEE J. Quantum Electron.* **37**(3), 322–328 (2001).
9. F. Litvack, "Role of laser and thermal ablation devices in the treatment of vascular diseases," *Am. J. Cardiol.* **61**(14), 81G–86G (1988).
10. J. T. Au et al., "Flexible CO(2) laser and submucosal gel injection for safe endoluminal resection in the intestines," *Surg. Endosc.* **26**(1), 47–52 (2012).
11. M. Ivanenko et al., "Ablation of hard bone tissue with pulsed CO_2 lasers," *Med. Laser Appl.* **20**(1), 13–23 (2005).
12. J. Neev et al., "Dentin ablation with three infrared lasers," *Laser Surg. Med.* **18**(2), 121–128 (1996).
13. T. Watanabe et al., "Synchronous radiation with Er:YAG and Ho:YAG lasers for efficient ablation of hard tissues," *Biomed. Opt. Express* **1**(2), 337–346 (2010).
14. J. I. Youn, P. Sweet, and G. M. Peavy, "A comparison of mass removal, thermal injury, and crater morphology of cortical bone ablation using wavelengths 2.79, 2.9, 6.1, and 6.45 mu m," *Laser Surg. Med.* **39**(4), 332–340 (2007).
15. M. Ooe et al., "Comparative evaluation of wrinkle treatments," *Aesth. Plast. Surg.* **37**(2), 424–433 (2013).
16. C. C. Wang et al., "Treatment of cosmetic tattoos using carbon dioxide ablative fractional resurfacing in an animal model: a novel method confirmed histopathologically," *Am. Soc. Dermatol. Surg.* **39**(4), 571–577 (2013).
17. M. Papadaki et al., "Vertical ramus osteotomy with Er:YAG laser: a feasibility study," *Int. J. Oral Maxillofac. Surg.* **36**(12), 1193–1197 (2007).
18. L. D. Rybak et al., "Thermal ablation of spinal osteoid osteomas close to neural elements: technical considerations," *Am. J. Roentgenol.* **195**(4), W293–W298 (2010).
19. D. Tucker et al., "Morphologic changes following in vitro CO_2 laser treatment of calculus-ladened root surfaces," *Laser Surg. Med.* **18**(2), 150–156 (1996).
20. K. Fan, P. Bell, and D. Fried, "Rapid and conservative ablation and modification of enamel, dentin, and alveolar bone using a high repetition rate transverse excited atmospheric pressure CO_2 laser operating at $\lambda = 9.3$ μm," *J. Biomed. Opt.* **11**(6), 064008 (2006).
21. W. B. Armstrong et al., "Ultrashort pulse laser ossicular ablation and stapedotomy in cadaveric bone," *Laser Surg. Med.* **30**(3), 216–220 (2002).
22. B. Girard et al., "Effects of femtosecond laser irradiation on osseous tissues," *Laser Surg. Med.* **39**(3), 273–285 (2007).
23. A. V. Rode et al., "Subpicosecond laser ablation of dental enamel," *J. Appl. Phys.* **92**(4), 2153–2158 (2002).
24. B. Emigh et al., "Porcine cortical bone ablation by ultrashort pulsed laser irradiation," *J. Biomed. Opt.* **17**(2), 028001 (2012).
25. J. Aerssens et al., "Interspecies differences in bone composition, density, and quality: potential implications for in vivo bone research," *Endocrinology* **139**(2), 663–670 (1998).
26. A. Borowiec and H. K. Haugen, "Femtosecond laser micromachining of grooves in indium phosphide," *Appl. Phys. A* **79**(3), 521–529 (2004).
27. S. Erkan et al., "Alignment of pedicle screws with pilot holes: can tapping improve screw trajectory in thoracic spines?," *Eur. Spine J.* **19**(1), 71–77 (2010).
28. R. J. Minns, "Surgical instrument design for the accurate cutting of bone for implant fixation," *Clin. Mater.* **10**(4), 207–212 (1992).
29. R. An et al., "Laser micro-hole drilling of soda-lime glass with femtosecond pulses," *Chin. Phys. Lett.* **21**(12), 2465–2468 (2004).
30. B. V. Ventura et al., "Role of optical coherence tomography on corneal surface laser ablation," *J. Ophthalmol.* **2012**, 676740 (2012).
31. J. Lee, O. B. Ozdoganlar, and Y. Rabin, "An experimental investigation on thermal exposure during bone drilling," *Med. Eng. Phys.* **34**(10), 1510–1520 (2012).